Available online at www.sciencedirect.com
SCIENCE DIRECT®
International Journal of Heat and Mass Transfer 48 (2005) 3560–3573
International Journal of HEAT and MASS TRANSFER
www.elsevier.com/locate/ijhmt

Optimization of a thermal manufacturing process: Drawing of optical fibers

Xu Cheng, Yogesh Jaluria *

Department of Mechanical and Aerospace Engineering, Rutgers, The State University of New Jersey, Piscataway, NJ 08854, United States

Received 14 October 2004; received in revised form 5 March 2005
Available online 26 May 2005

Abstract

The optimization of thermal systems and processes has received much less attention than their simulation and often lags behind optimization in other engineering areas. This paper considers the optimization of the important thermal manufacturing process involved in the drawing of optical fibers. Despite the importance of optical fibers and the need to enhance product quality and reduce costs, very little work has been done on the optimization of the process. The main aspects that arise in the optimization of such thermal processes are considered in detail in order to formulate an appropriate objective function and to determine the existence of optimal conditions. Using validated numerical models to simulate the thermal transport processes that govern the characteristics of the fiber and the production rate, the study investigates the relevant parametric space and obtains the domain in which the process is physically feasible. This is followed by an attempt to narrow the feasible region and focus on the domain that could lead to optimization. Employing standard optimization techniques, optimal conditions are determined for typical operating parameters. The study thus provides a basis for choosing optimal design conditions and for more detailed investigations on the feasibility and optimization of this complicated and important process.

Keywords: Optimization; Thermal systems; Optical fiber; Thermal manufacturing

1. Introduction

The demand for high quality optical fiber at reduced costs is pushing the design limits of the current fiber drawing technology. Various efforts are being directed at improving the fiber manufacturing system, with the goal of producing new and higher quality products at increased production rates and, thus, at lower cost. Optimizing the thermal system for fiber drawing is an important consideration in this effort. To optimize the fiber drawing process, careful formulation of the optimization problem and the use of an appropriate optimization technique, coupled with accurate numerical modeling, are needed.

Even though the importance of optimizing fiber drawing systems has been cited by many investigators, much of the research has been limited to the description and simulation of the physical behavior of the process

* Corresponding author. Tel.: +1 732 445 3652; fax: +1 732 445 3124.
E-mail address: jaluria@jove.rutgers.edu (Y. Jaluria).

0017-9310/$ - see front matter © 2005 Elsevier Ltd. All rights reserved.
doi:10.1016/j.ijheatmasstransfer.2005.03.012

Nomenclature

C_p	specific heat at constant pressure
E_d, E_p	activation energies in Eq. (7)
F	general function to be optimized
F_T	draw tension
g	magnitude of gravitational acceleration
H	mean surface curvature
K	thermal conductivity
k	Boltzmann constant
L	height of furnace; length of fiber
n_d, n_{p0}	concentration of E' defects and initial precursors, respectively
R	radius of preform, fiber, furnace
r	radial coordinate distance; absolute tolerance in Eq. (17)
S_r	radiative source term
t	time; parameter in Eq. (16)
T	temperature
T_m	glass softening point, typically around 1900 K for silica glass
u	radial velocity
U	objective function for fiber drawing
v	axial velocity
X	independent variable
z	axial coordinate distance

Greek symbols

δ	absolute tolerance in X
μ	dynamic viscosity
ν	kinematic viscosity
$\bar{\nu}$	frequency factor in Eq. (7)
Φ	viscous dissipation
ρ	density
ζ	surface tension between glass and purge gas

Subscripts

f	fiber
F	furnace
l	lower
lag	difference in values at center and surface
u	upper

[1–3]. Among the large number of simulation and experimental studies, very few have applied the results to the optimal design of the fiber drawing system. As an example, Nicolardot and Orcel [4] recently reported design work on the draw furnace by maximizing the thermal efficiency, using commercially available software. At the same time, feedback control systems, coupled to a fiber drawing system, have also received some attention. Both experimental measurements on a draw tower and numerical simulations of the drawing process can be used to provide the basis for an appropriate feasible design [5]. Mirho [6] developed a measurement-based feedback system to compensate for variations in draw speed, feed rate and draw diameter during the drawing process and to achieve the desired fiber quality, consistency and efficiency.

Compared to numerical techniques, experimental work for optimization is obviously very time consuming and expensive. Usually, only a small number of runs and a fairly limited design space exploration are possible. However, validated and accurate numerical models of the flow and the heat transfer, coupled to a proper optimization algorithm, can be effectively used for design, as has been done for other thermal manufacturing systems [7].

Since not much effort has been directed at the optimization of the fiber drawing system, there is a strong need for determining appropriate optimization procedures and for an efficient coupling of optimization techniques to the transport models. A preliminary study is carried out here to examine the possibility of optimization of the furnace-drawing system for optical fiber fabrication. Due to the complexity of the problem, essentially no prior optimization efforts are available in the reference. Therefore, the first goal of this work is to investigate the possibility of optimization and to give guidelines for the formulation and selection of an objective function based on the current understanding of the behavior of the system. The optimization procedure employs an objective function, which characterizes the fiber quality, productivity and operational costs, based on important measures indirectly derived from the drawing parameters, such as draw temperature, draw speed and heat-zone length. The general characteristics of the objective function being optimized are then examined using simple exhaustive search and curve-fitting techniques. A much larger parameter space, than that considered earlier, is based on existing knowledge of the feasible domain [5]. Automation of the optimization procedure using univariate search and Golden-section algorithm is then pursued.

A typical fiber drawing furnace, shown in Fig. 1, is used for the investigation. The neck-down shape of the fiber is iteratively obtained as a result of the force balance at the free surface. Optimal operation conditions are determined within the initially known feasible parameter space, followed by evaluation of the optimal conditions using the Golden-section method for univariate search to obtain a global minimum based on a chosen objective function.

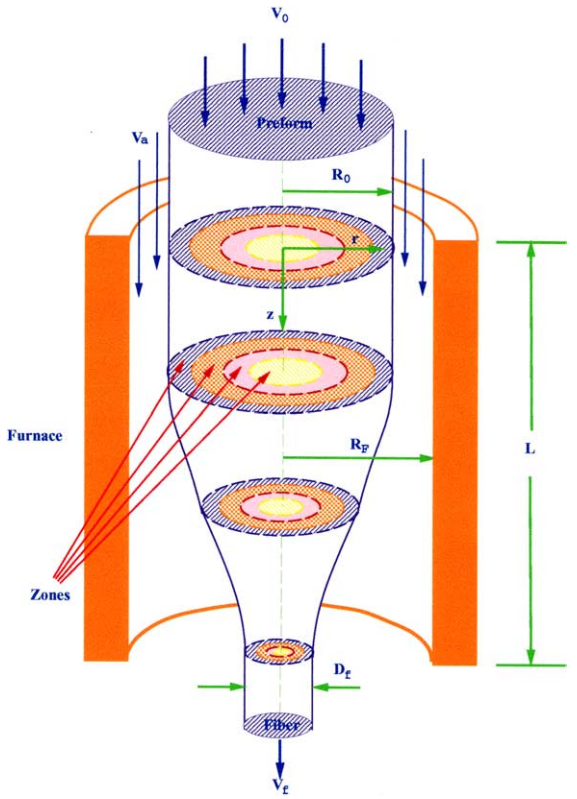

Fig. 1. A typical optical fiber manufacturing system.

2. Analysis and numerical solution

The transport phenomena in a cylindrical graphite furnace have been investigated for high-speed optical fiber drawing. A conjugate problem involving the glass and the purge gases is considered. Laminar flow is assumed due to the high-viscosity of glass and the typical low velocities of the gas flow. The transport in the two regions is coupled through the boundary conditions at the free surface. Thus, coupled conduction, convection and radiation heat transfer mechanisms are involved in the analysis. Several earlier papers have presented the analysis and the numerical scheme [8–14] and only a few important aspects are included here for completeness. For further details, these references may be consulted.

The governing equations for axisymmetric conditions, developed in cylindrical coordinates for both the glass and the purge gas, are given as [15]:

$$\frac{\partial v}{\partial z}+\frac{1}{r}\frac{\partial (ru)}{\partial r}=0 \tag{1}$$

$$\frac{\partial v}{\partial t}+u\frac{\partial v}{\partial r}+v\frac{\partial v}{\partial z}=-\frac{1}{\rho}\frac{\partial p}{\partial z}+\frac{1}{r}\frac{\partial}{\partial r}\left[rv\left(\frac{\partial v}{\partial r}+\frac{\partial u}{\partial z}\right)\right]+2\frac{\partial}{\partial z}\left[v\left(\frac{\partial v}{\partial r}\right)\right] \tag{2}$$

$$\frac{\partial u}{\partial t}+u\frac{\partial u}{\partial r}+v\frac{\partial u}{\partial z}=-\frac{1}{\rho}\frac{\partial p}{\partial r}+\frac{2}{r}\frac{\partial}{\partial r}\left(rv\frac{\partial u}{\partial r}\right)+\frac{\partial}{\partial z}\left[v\left(\frac{\partial v}{\partial r}+\frac{\partial u}{\partial z}\right)\right]-\frac{2vu}{r^2} \tag{3}$$

$$\rho C_p\left(\frac{\partial T}{\partial t}+u\frac{\partial T}{\partial r}+v\frac{\partial T}{\partial z}\right)=\frac{1}{r}\frac{\partial}{\partial r}\left(rK\frac{\partial T}{\partial r}\right)+\frac{\partial}{\partial z}\left(K\frac{\partial T}{\partial z}\right)+\Phi+S_r \tag{4}$$

where the viscous dissipation term, Φ, is given by

$$\Phi=\mu\left\{2\left[\left(\frac{\partial u}{\partial r}\right)^2+\left(\frac{u}{r}\right)^2+\left(\frac{\partial v}{\partial z}\right)^2\right]+\left(\frac{\partial u}{\partial z}+\frac{\partial v}{\partial r}\right)^2\right\} \tag{5}$$

Here, S_r is the radiative source term. The viscous dissipation and the radiative source terms are only kept for the glass flow due to their relative importance. The material properties, particularly glass viscosity, are strongly temperature dependent. A band model is used for approximating the radiative absorption coefficient of glass [16–18]. Thus, the equations are coupled because of property variation and viscous dissipation. For the convenient implementation of the finite difference method, the flow domains for the glass and purge gas are transformed into cylindrical ones [15,19]. The boundary conditions for a free surface, arising from the force balance, are employed here at the interface between the glass and the purge gas in order to determine the neck-down profile. A more detailed discussion about the governing equations and the boundary conditions can be found in the preceding references.

Draw tension, which is crucial to fiber quality and process feasibility, is determined by considering the contribution of the viscous force, surface tension, inertia force and gravity, resulting in the equation:

$$F_T=3\pi\mu R^2\frac{\partial u}{\partial z}+\pi R^2\zeta H+\pi\rho\int_z^L R^2u\frac{\partial u}{\partial z}\,dz-\pi\rho g\int_z^L R^2\,dz \tag{6}$$

where the forces acting at a horizontal cross-section of the preform/fiber are considered to determine the draw tension. A low value of the tension is desirable from fiber quality considerations and a large value could result in viscous rupture of the fiber [8,13].

A thermally induced defect, known as the E' point defect, is generated due to the breaking of the bond between silicon and oxygen and is of particular interest in fiber quality. The generation of these defects is strongly dependent on the temperature history of the fiber. The defect generation–recombination process is analyzed by the model given by Hanafusa et al. [20], on the basis of the thermodynamics of lattice vacancies in crystals,

and the resulting defect concentrations in the fiber are calculated. The equation, modified to a point mass moving along the streamline, is:

$$v\frac{dn_d}{dz} = n_{p0}\bar{\nu}\exp\left(-\frac{E_p}{kT}\right) - n_d\bar{\nu}\left[\exp\left(-\frac{E_p}{kT}\right) + \exp\left(-\frac{E_d}{kT}\right)\right] \quad (7)$$

where, n_d is the concentration of E' defects, and n_{p0} is the concentration of the initial precursors, E_d and E_p are corresponding activation energy of these, $\bar{\nu}$ is the frequency factor, and k the Boltzmann constant. The values of the constants are given by Hanafusa et al. [20]. For pure silica, the initial concentration of E' defects is taken as zero. Thus, using this kinetics equation, the concentration of defects at various locations in the preform/fiber can be calculated.

The radiation transfer is a volume phenomenon in semi-transparent glass and the zonal model is used to compute the radiative source term. Details of the method and the radiative properties used are given in [16–18]. In order to avoid computation of the direct exchange areas every time the neck-down profile is corrected, since this is very time-consuming, the optically thick approximation is first used to generate the neck-down profile [21,22]. This profile is used as the initial guess to generate the final neck-down profile with the zonal method. This strategy is based on the observation that the difference between the results obtained by using the optically thick approximation and by the zonal method is moderate. The neck-down profile is corrected after every 4–10 thousand steps of temperature and velocity calculations, in order to reduce the CPU time. Thus, each iterative step in the neck-down profile determination involves substantial computational effort.

The conjugate problem, outlined above, is solved by a finite difference method, using the alternating direction implicit (ADI) scheme [23]. Two discretization schemes are used. A finer one is adopted for the stream function, vorticity and energy equations and a coarser one for the radiation analysis using zonal method. Non-uniform grids are employed for the transport equations because of dramatic changes in the physical variables, particularly viscosity. Finer grids are used wherever large velocity and temperature gradients are expected. The optimal grid sizes for all cases are experimentally determined by obtaining mesh-independent results. For a 5 cm diameter and 50 cm long preform in a 7 cm diameter furnace, a grid-optimization study resulted in a 669×41 (axial and radial, respectively) non-uniform grid in the preform/fiber and 669×61 non-uniform grid in the purge gas. The radiation grid is also obtained as 51×6. Because the radiation grid is coarser than that for the energy equation, the radiative source term at the grid points for the energy equation is obtained by bi-linear interpolation from the results at the radiation grid points. The convergence to steady state conditions is indicated by the invariance of all the physical variables. This is ensured by the infinite norm of the change in all physical variables between adjacent iterations becoming less than a prescribed convergence criterion. The criterion was varied to ensure that results are independent of the values chosen. The optimal criteria may change somewhat depending on the drawing conditions, i.e. the drawing speed, the drawing temperature, and the dimensions of glass preform and draw furnace.

The analytical and numerical modeling was validated by comparisons with earlier results on optical fiber drawing. Experimental results at relatively low draw speeds of up to 3 m/s and for isothermal and parabolic temperature distributions for relatively short furnaces of length around 30 cm were employed. Several of these comparisons have been given in earlier papers [13,21,24,25] and are not repeated here for conciseness.

3. Existence of optimal conditions

Optimization of the system and the process involves determination of optimal drawing conditions that minimize fiber defects, while keeping the productivity high. Due to the complexity of the physical problem, very little work is available to guide the optimal design of the fiber drawing system in actual practice. However, the first question to be answered by observations of the behavior of a fiber drawing system is if it is possible to optimize such a process, which is defined by the drawing parameters such as draw temperature, draw speed and furnace dimensions.

The effect of draw furnace dimensions is first investigated. The heat zone length is varied from 25 to 50 cm, while the furnace diameter is kept as 7 cm. A parabolic temperature profile with maximum of 2500 K in the middle and minimum of 2000 K at the two ends is prescribed at the furnace wall. The dimensionless temperature profile is kept the same for all furnace lengths. Two draw speeds, 15 and 25 m/s, are considered for comparison. Constant properties are assumed for the aiding Argon gas flow at 0.1 m/s. Both the preform and the purge gas are assumed to enter the furnace at 300 K. These values are chosen from typical operating conditions for fiber drawing on medium-sized, graphite furnace, draw towers, one such tower being available to us for experimentation [24,25].

It is known that the temperature difference, or lag, between the surface and the centerline describes the thermal response in the glass. Fig. 2(a) shows the variation of the maximum temperature lag in the drawing process. It is seen that the heating zone length affects the lag level only slightly. But, the influence of draw speed is quite significant. The difference between the surface and

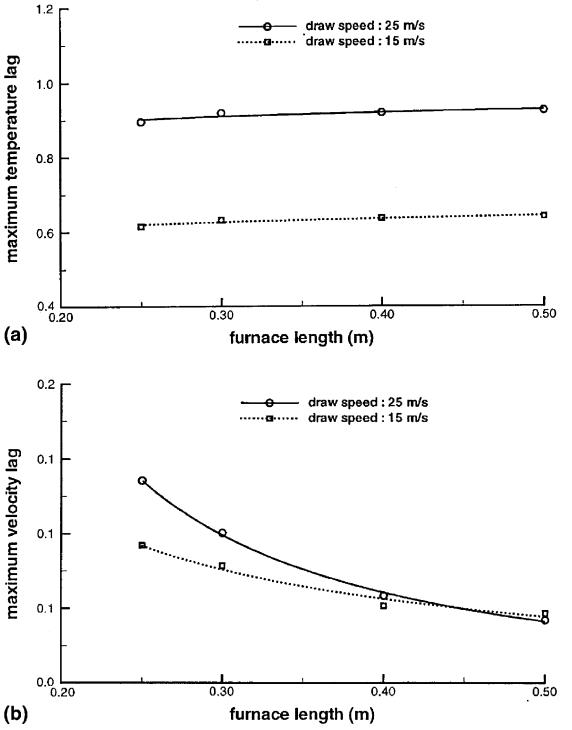

Fig. 2. Maximum (a) temperature, and (b) velocity difference, or lag, between glass surface and centerline.

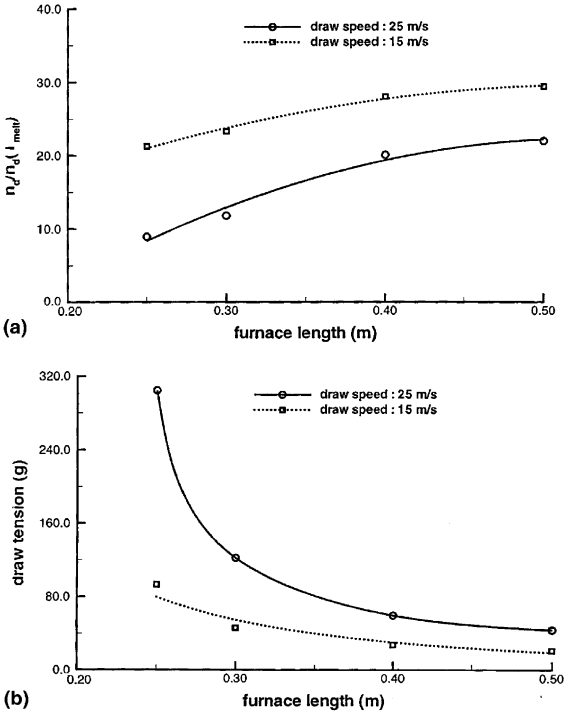

Fig. 3. Dependence of (a) average concentration of E' defects at the furnace exit, and (b) draw tension on furnace length at two draw speeds.

centerline temperatures increases about 30% when the draw speed goes up from 15 m/s to 25 m/s. This result suggests that the residence time of the glass rod inside the heating furnace is the dominating factor in controlling the radial temperature difference, since a longer residence time causes the preform to be more uniformly heated. Additional results also show that the temperature lag in the fiber is basically dominated by the conditions at the furnace entrance and preform diameter, rather than by the thermal evolution inside the draw furnace.

The radial non-uniformity in the temperature in the preform noticeably affects the velocity field, because glass viscosity is an exponential function of the temperature [15–17]. This can cause the redistribution of the material dopants and impurities and, therefore, impact the fiber quality [13,20,22]. The variation of the maximum velocity lag in the neck-down region is shown in Fig. 2(b). Interestingly, the velocity lag is very sensitive to the furnace dimensions. The lag decreases significantly with an increase in the furnace length. The difference at the two draw speeds is large only for shorter furnaces, and diminishes as the heating zone increases.

Fig. 3(a) shows the average concentration of E' defects in the fiber at the furnace exit. The defect concentration monotonically increases with an increase in the heating zone length and with a decrease in the draw speed. It is because a longer residence time of fiber inside the heating furnace will cause more frequent occurrences of Si–O bond breakage in the precursors. The draw tension strongly affects optical and mechanical properties of the fiber in terms of index of refraction, residual stresses, and transmission losses, ultimately influencing the fiber strength and optical quality. A draw tension kept under a specified threshold is critical to achieving continuous pulling of optical fibers without breakage [26]. Fig. 3(b) shows the dependence of draw tension on the furnace length and draw speed. It is found that the draw tension decreases dramatically with an increase in the furnace length for a given temperature profile. The reason is that a longer heating zone gives rise to relatively smaller rate of change of radius with distance and the viscosity also changes more gradually. Therefore, the draw tension is reduced. This result also indicates that a moderate furnace length is desirable to achieve low fiber tension particularly for high-speed fiber drawing. From the figure, it is also found that a high draw speed can cause a high draw tension.

From these results, it is very interesting to point out that the heat-zone length and draw speed demonstrate opposite effects on the fiber quality, especially in terms of velocity lag, defect concentration, and draw tension. This observation strongly suggests the existence of a

trade-off between draw speed, which determines the production rate, and furnace dimensions in order to balance the requirements of quality and productivity in the fiber fabrication process.

The dependence of the preform/fiber characteristics on the draw temperature is only investigated for a typical draw speed of 15 m/s. A fixed furnace length of 30 cm is employed. The imposed temperature profile is still parabolic while only the maximum temperature at the mid-point of the furnace is changed, ranging from 2200 K to 3000 K.

The maximum temperature and velocity lag in the glass are shown in Fig. 4. It is seen that the temperature lag decreases slightly when the draw temperature increases. The velocity lag variation with the draw temperature shows a minimum. The lag levels are all above 30% at the two extreme draw temperatures of 2200 K and 3000 K. However, the reasons for this are a little different. The former temperature almost reaches the lower temperature boundary of the feasible drawing domain for the given furnace, and, therefore, the weak heat input at the glass surface results in slow thermal response at the center. On the contrary, a temperature as high as 3000 K causes a rapid change in velocity at the glass surface due to the intense heat flux applied there. However, the effect does not propagate to the center immediately due to thermal inertia.

Fig. 5(a) shows the generation of E' defects in the fiber for different maximum furnace temperatures. These defects in the fiber are very sensitive to the drawing temperature. The average defect concentration at the furnace exit increases by almost two orders in magnitude when the draw temperature goes up from 2200 K to 3000 K. This result suggests that minimizing the drawing temperature is not only desired for increasing the lifespan of the draw furnace, but also for decreasing the point defects in the optical fiber to an acceptable level. The variation of draw tension with the draw temperature is shown in Fig. 5(b). Due to the exponential dependence of the glass viscosity on the temperature, the draw tension decreases dramatically with the increase of the furnace temperature. Thus, increasing the draw temperature becomes important for tension control.

These results show that most physical variables characterizing the quality of the fibers depend strongly on the dimensions and temperature of the heating furnace. In terms of thermal and geometrical configuration, the optimum design of the draw furnace is also possible by considering a trade-off between these characteristics. It is especially clear that a longer heating furnace with a higher temperature has a positive effect on the draw tension. However, the length and temperature of the furnace are obviously constrained by the dramatic increase in defect concentrations. Simultaneously, the

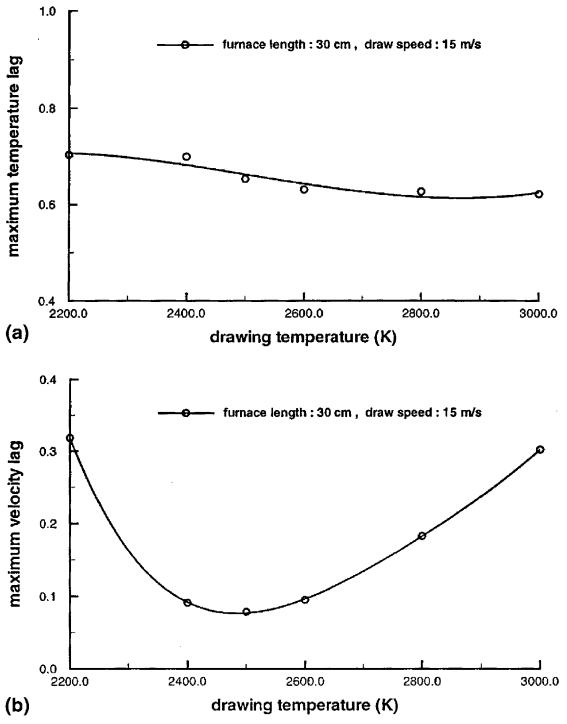

Fig. 4. Variation of maximum (a) temperature, and (b) velocity lag with the furnace wall temperature.

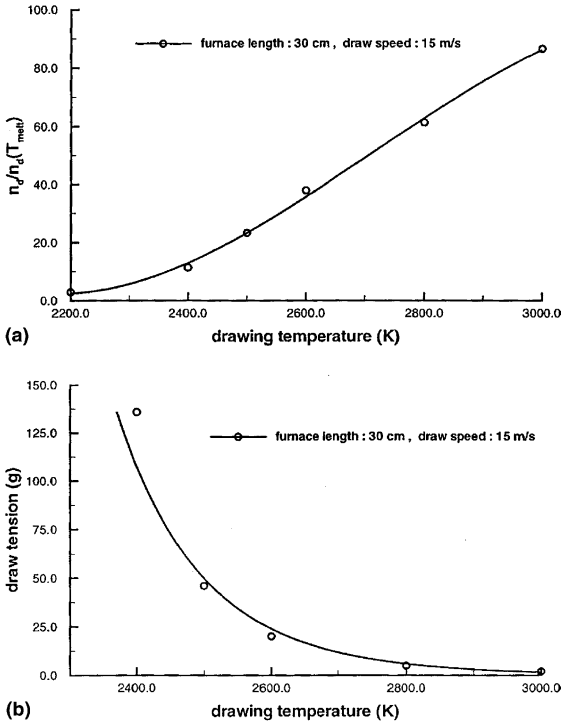

Fig. 5. Effect of the furnace wall temperature on (a) the average concentration of E' defects, and (b) the draw tension.

change in radial uniformity also becomes a concern for the best fiber performance.

Overall, the previous observations indicate that optimization of the drawing conditions, as well as optimal design of the draw furnace, for high-speed optical fiber drawing can be achieved by constructing an objective function from velocity lag, defect concentration and draw tension, since the temperature lag is not very sensitive to variations in the drawing conditions over the ranges considered here.

4. Formulation of objective function

The design and optimization of the fiber drawing system follows well-established procedures for thermal systems, as described by Jaluria [27]. System requirements, design variables and constraints can be selected for the process under consideration.

A number of parameters, specified as design variables, are to be varied to satisfy a number of system requirements. These variables cover both the hardware and the operating conditions. The hardware includes the geometry and the dimensions of the furnace, arrangement of the heating and cooling zones, flow configuration for the purge gas, and other system parameters. The operating conditions include variables, which can usually be changed without varying the hardware. These include draw speed of the fiber, or feed rate of the preform, heat-zone temperature or heat input at the furnace wall, composition and flow rate of the purge gas and inlet temperature conditions of the preform and the purge gas. Although the design variable list could be much larger, most hardware variables are predetermined and generally kept fixed for a typical fiber drawing system. A sensitivity analysis is used to determine the dominant quantities. Operating conditions can be further simplified by considering the most important variables. System constraints are typically physical limitations and conservation principles that arise in thermal systems, such as conservation of mass and energy and momentum–force balance, temperature and stress limitations of the materials, flow limitations and others.

Using the description of the problem, as given earlier, we can proceed to determine the main quantities of interest. For the fiber drawing system shown in Fig. 1, quantities of interest include product quality (Q) or defect in the product (D), production rate (P) and operating cost (C). However, there are many possibilities to formulate the objective function to be minimized or maximized. For instance, one possible formulation is obtained by writing the objective function (U) as the product of different design quantities. Thus,

$$U = \frac{\text{Operation cost}}{\text{Product quality} \times \text{Production rate}} \tag{8}$$

or,

$$U = \frac{\text{Operation cost} \times \text{Product defect concentration}}{\text{Production rate}} \tag{9}$$

These quantities are considered as independent variables, because it is difficult to determine the relationships between them in a fiber drawing system.

Unfortunately, several considerations make it very difficult to evaluate the operating costs for such a complicated system, even though the draw speed, v_f, is a good measure of the production rate of the fiber. Very little data are available to simply model the operating costs of a fiber drawing system for various drawing conditions. In addition, the evaluation of the system operation costs involves the heating rate and purge gas consumption inside the furnace, as well as the operation of the subsequent cooling and coating sections outside of the furnace. Any change in operating conditions, particularly draw speed and furnace temperature, will inevitably affect the technical and operational costs in the post-drawing procedures, even though the hardware of draw furnace is kept fixed.

In this study, the objective function is used to emphasize the product defects, i.e. product quality. A special defect index is chosen to characterize the quality of fiber product. As was mentioned earlier, three physical quantities, namely the maximum velocity lag, average E' defect concentration and average draw tension, quantify the mechanical and optical attributes of the fiber. After a detailed consideration of factors contributing to the objective function, an explicit form of the objective function can be proposed as given below. Then, the drawing conditions are taken as optimal, in terms of fiber quality, when the objective function reach a minimum.

$$U = \sqrt{\left(\frac{v_{\text{lag}}}{\bar{v}_{\text{lag}}}\right)^2 + \left(\frac{n_d}{\bar{n}_d}\right)^2 + \left(\frac{F_T}{\bar{F}_T}\right)^2} \tag{10}$$

This form of the objective function represents equal weighting for each dimensionless design quality, i.e. it is assumed that all three factors contribute equally to the design. However, each physical variable is scaled by a reference value, which is empirically picked from a well-known threshold or a physically significant reference point. For example, the reference for draw tension, $\bar{F}_T$ is set as 150 g, which is a tension threshold of continuous fiber drawing in practice. The scale, $\bar{n}_d$, is the E' defect concentration of fiber at a static and equilibrium state of 2000 °C. The reference value for radial velocity lag, $\bar{v}_{\text{lag}}$, is chosen as 0.25. This is a reasonable threshold that indicates significant velocity lag and thus requires a 2-D or a 3-D model, instead of a simple lumped model, to solve the velocity distribution and obtain an accurate neck-down profile.

It is clear that the optimal drawing conditions may change due to the empirical choice of these reference values. However, this arbitrariness cannot change the fact that the fiber drawing conditions can be optimized based on the proper formulation and design of the application. Also, different criteria for optimization can be considered separately in order to develop a strategy for multi-criteria optimization of the process.

We need to emphasize two additional points. First, the quantities employed in constructing the objective function can be combined in other ways, for example, weighting these using exponentials. For this study, the proposed simple form of the objective function is sufficient to demonstrate the feasibility of optimization of a fiber drawing system. Second, the temperature lag, a possible design quality, is screened out from our formulation by a sensitivity analysis. Another reason for neglecting it is that it is strongly dependent on the inlet thermal boundary conditions, as discussed earlier, and these are not changed here.

All the design qualities in the objective function implicitly depend on two important drawing parameters, i.e. draw speed v_f and draw temperature T_F. Therefore, these parameters are chosen as the design variables to optimize the fiber drawing system. Due to the physical limitations and constraints on the fiber and draw furnace, these two design variables are limited to the following ranges in which fiber drawing is numerically and practically feasible:

Draw temperature:

$$2200\ \mathrm{K} \leqslant T_F \leqslant 3000\ \mathrm{K} \tag{11}$$

Draw speed:

$$1\ \mathrm{m/s} \leqslant v_f \leqslant 30\ \mathrm{m/s} \tag{12}$$

Therefore, optimum operating conditions are to be determined in this domain of parameters.

The possibility of optimizing the draw furnace is also discussed in terms of the heat zone length later. The range of furnace length L used for typical drawing conditions is:

Furnace length:

$$0.25\ \mathrm{m} \leqslant L \leqslant 0.5\ \mathrm{m} \tag{13}$$

5. Optimization algorithm

Search methods, which are based on selecting the best design from the acceptable space, are among the most widely used methods for optimizing thermal system. Search methods are used for a wide variety of problems, ranging from simple problems with unconstrained single-variable optimization to extremely complicated systems with multiple constraints and variables.

There are several approaches that can be employed in search methods, depending on whether the problem considered is a constrained or an unconstrained one, and whether it involves a single variable or multiple variables. In elimination methods, the uncertainty domain, in which the optimum lies, is gradually reduced to a desired level by eliminating regions that are determined not to contain the optimum. The initial interval of uncertainty is defined by the acceptable ranges of the variables. The Golden-section method is one of the search schemes based on elimination for single-variable problems [27]. Hill-climbing techniques involve trying to find the shortest way to the maximum or minimum of the objective function. This approach is more involved than the elimination methods, but generally more efficient in terms of convergence. Univariate search, an extension of elimination methods for multivariable problems, is one of the widely used hill-climbing techniques because of its simplicity [28–30].

Since at least two design variables are involved in a typical fiber drawing system, univariate search is first used for this study to divide the multivariable problem into two single-variable problems. Golden-section method is then employed to automate the optimum search for each simple problem.

5.1. Curve fitting in optimization

Curve fitting is a useful approach to obtain the optimum in many optimization analyses. It is assumed that the behavior of the objective function can be described by a simplified, continuous, and differentiable curve in the given domain. Polynomial functions are commonly employed for the curve fitting. The optimum can then easily be found from the determination of the minimum or maximum point in the curve, where the first derivative of objective function is equal to zero.

Curve fitting can also be used to reveal the general characteristics of the objective function being optimized and therefore it is useful for circumstances where the basic trends of the objective are not known because of the complexity of the problem or because it is a new problem with little prior information. Optimization of the fiber drawing system is one of these cases. The effects of drawing parameters are not easy to predict due to the dependence of system behavior on the fiber material, whose properties vary strongly with temperature and are then affected by the flow and heat transfer process. Thus, the curve fitting approach can be used to initially determine the behavior of the objective function by employing a small number of runs. An automated approach can be considered later, using the obtained information, if the computational cost is acceptable. However, the curve-fitting method is essentially an exhaustive search method, which is not an efficient

strategy to determine the optimum, since it covers the entire domain uniformly.

5.2. Golden-section method for single-variable optimization

The Golden-section method is a popular and automated algorithm to numerically solve the optimization problems for functions of one variable [27–30]. It uses the well-known Golden ratio, 0.618, to locate the trial runs in the search for the optimum. The strength of this method is that the accuracy and convergence of the scheme can be guaranteed. However, the weakness is the relatively large number of function evaluations necessary to reach the solution. The algorithm is given in Fig. 6. In this figure, F represents the objective function to be optimized with the independent variable X. X_l and X_u are the lower and upper bounds, respectively. F_l and F_u are the corresponding values of the evaluated function. Two intermediate points X_1 and X_2 ($X_1 < X_2$) are picked according to the following relations:

$$X_1 = (1-t)X_l + tX_u \tag{14}$$

and

$$X_2 = tX_l + (1-t)X_u \tag{15}$$

where t is

$$t = \frac{3-\sqrt{5}}{2} = 0.38179 \tag{16}$$

F_1 and F_2 are the function values at these intermediate points.

An acceptable solution for this method is controlled by a relative tolerance, r, which is defined by the ratio of an absolute tolerance in X, δ, and the initial interval.

$$r = \frac{\delta}{X_u - X_l} \tag{17}$$

By recognizing that the interval is reduced by a fraction θ on each iteration, an easy way to ensure convergence is to convert the tolerance r to a maximum number of function evaluations, in addition to the three that are required to evaluate F_l, F_l and F_u. The total number of function evaluations, N, in the iterative procedure can be given as:

$$N = \frac{\ln(\delta)}{\ln(1-\theta)} + 3 = -2.078\ln(\delta) + 3 \tag{18}$$

From above expression, it is easy to determine that 10 iterations in total are needed to reduce the interval to less than 5% of the initial one.

After the interval satisfies the convergence criteria, the optimal value of design variable can be obtained by an average of the lower and upper bounds of the new interval:

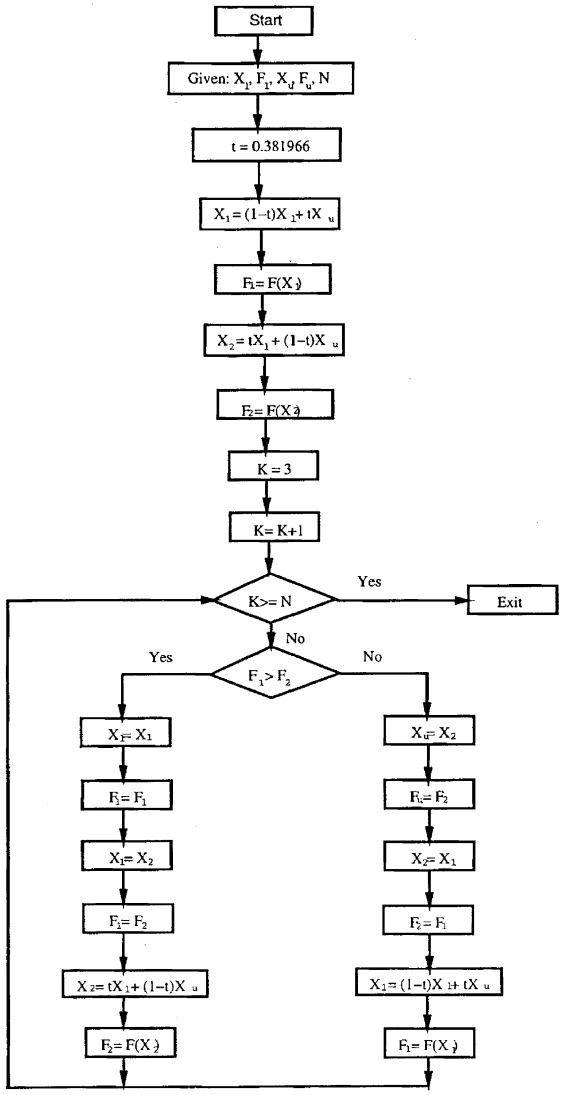

Fig. 6. Golden-section optimization algorithm.

$$X_{opt} = (X_1 + X_u)/2 \tag{19}$$

The Golden-section method to optimize one-variable function is popular for several reasons. First, the function need not have continuous derivatives due to the unimodality assumption. Secondly, the rate of convergence for the Golden-section method is known, as opposed to curve-fitting techniques. In addition, this method is pretty easy to program. Finally, it has been proved to be reliable for poorly conditioned problems. However, the negative aspect is that a relatively large number of function evaluations are needed.

Two assumptions are important in the theory for the development of above optimization algorithms. The function must be unimodal to find the optimum. That is, the function must have only one optimal value in

the region of our search. In addition, the functions are taken as continuous together with continuous first and second derivatives in the theory. It is known that, in practice, the unimodality and continuity assumptions are good for most applications.

5.3. Univariate search for multi-variable unconstrained optimization

A thermal system is normally governed by more than one independent variable. However, many practical thermal systems can be well characterized in terms of two or three dominant variables, because the complexity of the optimization problem rises dramatically as the number of variables increases [27]. As an example, a fiber drawing system may be taken as dominated by two parameters, i.e. draw temperature T_F and draw speed v_f, for a given drawing furnace with fixed dimensions.

Among many methods for multivariable, unconstrained optimization, univariate search is particularly useful for optimizing thermal systems with discrete values of the design variables [28,29]. Univariate search reduces the multivariable problem into a series of single-variable optimization problems by optimizing the objective function with respect to one variable at a time. For a system with two independent variables, one of the variables, x, is first held constant, and the function is optimized with respect to the other variable y in the feasible domain. After the optimum with respect to y is obtained, y is held constant at the optimal point and the function is then optimized with respect to x. This optimization procedure is repeated by alternating the independent variables, until the overall optimum is obtained in terms of the specified convergence criterion. The Golden-section method can be used to solve the single-variable problem. Generally, a starting point for univariate search is chosen on the basis of available information on the system or as a point away from the boundaries of the region.

A univariate search may fail in certain circumstances, such as ridges and very sharp changes occurring in the objective function [29]. However, it is possible to overcome such difficulties by varying the starting point, interval of search and the single-variable search strategy.

Constrained multivariable problems are the most complicated ones encountered in the optimization of thermal systems. The inequality constraints generally define the feasible domain and the equality constrains often arise from conservation principles. Because of their complexity, efforts are made to include the constraints in the objective function, thus obtaining an unconstrained problem. In this study, the constraints are already used in the formulation and simulation of the fiber drawing system, and only a multi-variable, unconstrained optimization problem needs to be solved here.

6. Results and discussion

6.1. Optimal drawing conditions

In this section, the results on optimal drawing conditions are first considered on the basis of the univariate search and the Golden-section scheme. A typical draw furnace, with fixed dimensions, is used for the numerical experiments. The length of the heat zone is kept fixed at 30 cm, and the inner diameter at 7 cm. A parabolic temperature profile, with the maximum in the middle and minimum at the two ends, is prescribed at the inner wall of the draw furnace. The minimum temperature is set at 2000 K. The maximum temperature, as well as draw speed, are varied for determining the optimal conditions.

As discussed earlier, we have a multivariable, unconstrained optimization problem for the fiber drawing system, and the objective function is of the form given in Eq. (10). Univariate search is first used to reduce the multivariable problem into two single-variable optimization problems. The Golden-section method is afterwards employed to optimize the objective function with respect to one variable at a time. In this study, the objective function is initially optimized with respect to draw temperature in the feasible domain of Eq. (11) by holding the draw speed constant. The Golden-section search algorithm, described in Fig. 6, is used to solve this single-variable optimization procedure. After the optimum is obtained for draw temperature, the function is then optimized in a similar way with respect to draw speed, while keeping the draw temperature constant at the optimal point. This optimizing procedure is repeated by alternating the independent variables until the overall optimum is reached, as given by a specified convergence tolerance.

In this study, the optimum search originally starts at draw speed of 15 m/s. The relative convergence tolerances of the Golden-section search are set as 5% for draw speed and 2% for draw temperature because of the consideration of computational expense. From Eq. (18), such a tolerance means that at least 10 or 12 function evaluations are necessary to complete an optimum search procedure for the corresponding variable. It is very CPU expensive, because even one typical function evaluation, using neck-down profile calculations and the zonal method, costs more than 20 CPU hours on various high-performance computing facilities (including CRAY C90, CRAY T90, HP SPP2000 and SPP2200, Sun E10K, and a RCG Cluster). Therefore, at most one more step of optimum evaluation is tried for each independent variable, except the initial one. However, the results are good enough for us to test the applicability of our formulation and to learn more about the system behavior during the optimization procedure. In general, a global optimum is obtained in that

the optimums evaluated both by two design variables satisfy the given accuracy requirements.

Fig. 7 shows the evaluation procedure of the optimal draw temperature at a starting draw speed of 15 m/s. In this figure, all other available data from the previous studies are also presented except those evaluated using Golden-section search. Evolution of the search interval using Golden-section search is given in Fig. 8(a) for every iteration step. It is very interesting to see from the search path that the objective function behaves in such a consistent way that an optimum of the draw temperature is easy to determine from the trends. When the temperature goes up from 2200 K to 3000 K, the function dramatically decreases in value, first reaching a minimum and then gradually increasing. This trend can be explained in terms of Fig. 8(b). The draw tension becomes much more dominant compared to the defect concentration in the objective function because of the viscosity change in the fiber material at low drawing temperatures. On the other hand, the magnitude of draw tension decreases exponentially when the draw temperature increases and finally becomes a secondary effect, compared to the contribution of defect generation. It is because the defect concentration in the fiber is also very sensitive to the furnace temperature but changes in the opposite direction.

The optimal draw temperature at this step can be obtained as 2489.78 K by averaging the upper and lower bounds of the converged search interval [2484.51 K, 2495.04 K]. One thing to be emphasized is that the best trade-off between draw tension and defect generation is not the point of optimum due to the role of the maximum velocity lag in the objective function.

Fig. 9 shows the evaluations to search for the optimal draw speed at a fixed temperature of 2489.78 K, the optimal just obtained in the previous step. Fig. 10(a) also gives the evolution of the search interval at each step when Golden-section method is used. It is seen that

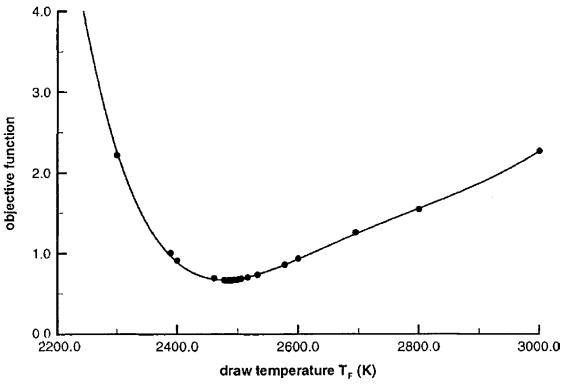

Fig. 7. Evaluation of the optimal draw temperature using Golden-section method at a draw speed of 15 m/s.

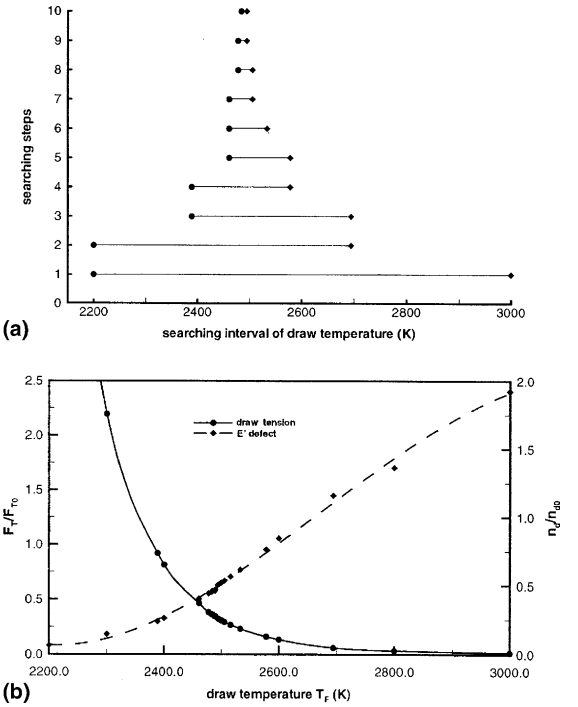

Fig. 8. (a) Iterative search interval of draw temperature using Golden-section method, and (b) variation of draw tension and E' defect concentration at a speed of 15 m/s.

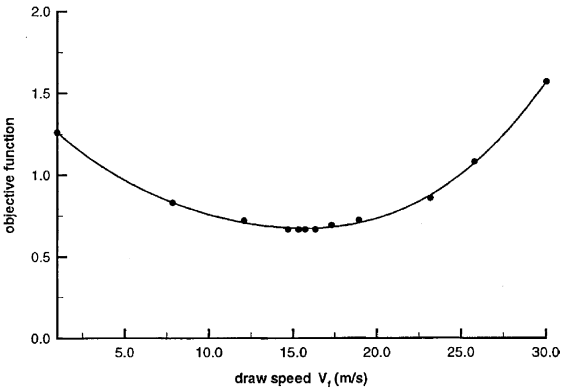

Fig. 9. Evaluation of the optimal draw speed using Golden-section method at a draw temperature of 2489.78 K.

the behavior of the objective function is basically parabolic when it is correlated to the independent variable of draw speed. Compared to the effects of draw tension, defect generation plays a more important role in fiber quality at lower draw speed, but more of a secondary effect at higher speed. This observation, seen in Fig. 10(b), can be explained by the variation of the residence time of the preform inside the heating furnace. As discussed earlier, this residence time is determined by the speed of

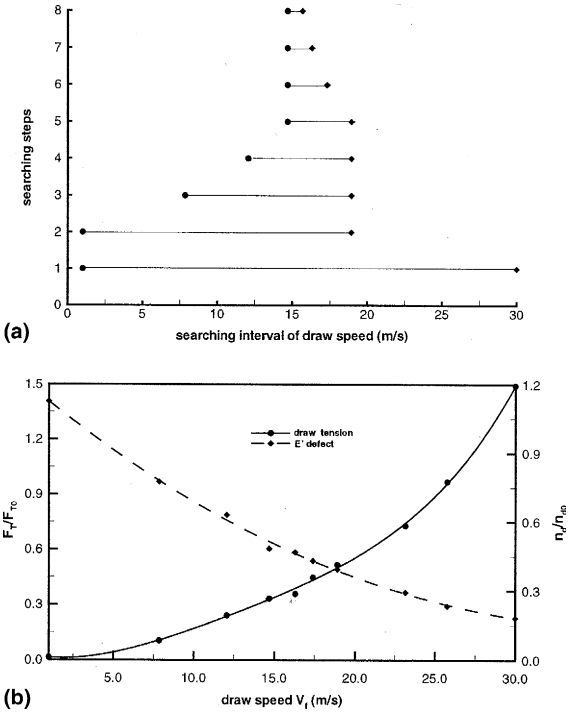

Fig. 10. (a) Iterative search interval of draw speed using Golden-section method, and (b) variation of draw tension and E' defect concentration at a draw temperature of 2489.78 K.

feed of the preform (or the draw speed of fiber), for a given furnace. As long as the preform resides for a longer time inside the heating furnace, it is more uniformly heated to a higher temperature and, therefore, demonstrates a significant difference in the level of draw tension and drawing-induced defects. From Figs. 8(b) and 10(b), it is also found the concentration of E' defects experiences a change of one order in magnitude for the complete search domain whatever the draw temperature or the draw speed. However, draw tension undergoes a change of two or more orders of magnitude in the same domain.

By comparing Fig. 7 with Fig. 9, it is also interesting to notice that the function value changes more sharply with the draw temperature than that with the draw speed. The objective function becomes especially insensitive to the draw speed at the bottom of the curve, which is around the optimal interval of [14.69 m/s, 15.69 m/s]. Due to this sensitivity difference, it is reasonable that a higher convergence tolerance of 5% is adopted for draw speed evaluation, instead of the value of 2% used for draw temperature.

An additional evaluation step is scheduled at the most recent optimal draw speed of 15.19 m/s in order to obtain a more accurate value of the optimal draw temperature. As expected, very similar results, as presented for 15 m/s, are observed for draw tension, defect concentrations, velocity lag and thus the objective function. A new temperature of 2483.27 K is found to be a better option. Since both draw temperature and draw speed have already converged to the optimal interval, in the sense of acceptable tolerance, a global optimal design of drawing conditions has been reached. For the given constraints of the fiber drawing system, a draw temperature of 2483.27 K and a draw speed of 15.19 m/s are the best drawing parameters in the feasible domain of Eqs. (11) and (12).

6.2. Optimal furnace dimension

Besides the efforts to determine optimal drawing conditions for a given furnace, it is also important to optimize the design of the draw furnace [31]. A draw furnace, with only the length taken as a design parameter, is discussed here for this preliminary study. An inner diameter of 7 cm is set for the furnace, while the heat zone length is varied between 25 and 50 cm. A parabolic temperature profile, with a maximum of 2500 K in the middle and a minimum of 2000 K at the two ends, is prescribed at the furnace wall. To compare the results, the dimensionless temperature profile is kept the same

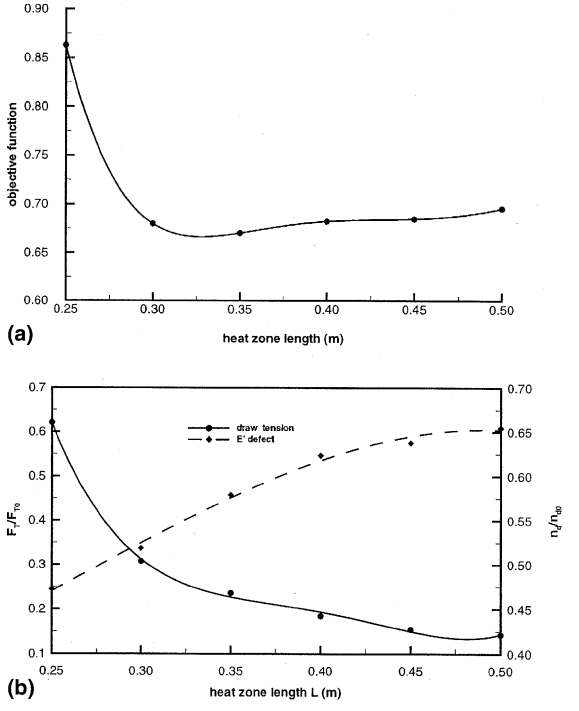

Fig. 11. (a) Evaluation of the optimal heat-zone length, and (b) variation of draw tension and E' defect concentration with the heat-zone length, at a draw temperature of 2500 K and a draw speed of 15 m/s.

for all the furnace lengths. A typical draw speed of 15 m/s is used for this consideration.

Employing the same objective function as given in Eq. (10), the curve-fitting method based on the available data is used to investigate the behavior of the objective function with respect to the heat zone length. Due to the high CPU time and the complexity of computational mesh adjustment, the Golden-section search is not considered. The objective function, curve fitted from the available computational data, is shown in Fig. 11(a). It is found that the objective function changes only slightly in the domain above 30 cm. Draw tension and defect concentration change by same order of magnitude, but in the opposite direction, as seen in Fig. 11(b). However the value rises sharply when the heating zone length gets too short in terms of the given drawing parameters, i.e. 2500 K in temperature and 15 m/s in speed. It is reasonable because a very short heat zone will reduce the residence time of the preform and decrease the heat input significantly. A much larger draw tension is thus caused, which contributes more to the value of objective function than the other factors. As a result, an optimal furnace length can be obtained between the 30 cm and 35 cm for the given drawing conditions.

7. Conclusions

As optimal design of the fiber drawing system is of great interest and demand in the optical fiber industry. Effective numerical models of the flow and thermal transfer, coupled with proper optimization algorithms, are very critical for achieving this goal. This work first investigates the possibility of the optimization of the drawing system. The results show that most physical variables, characterizing the quality of the fiber, strongly depend on the dimensions and temperature of the heating furnace. In terms of thermal and dimensional configuration, an optimal design of the draw furnace is possible by considering a trade-off between these aspects. As an example, a longer heating furnace with a higher temperature helps in the control of the draw tension. However, the length and temperature of the furnace are limited by the concentration of defects generated.

The formulation guidelines for the objective function are given next, based on our understanding to the behavior of the drawing system. The objective function, characterizing the fiber quality, is defined using the velocity lag, defect concentration and draw tension, which are all derived quantities dependent on the drawing parameters. Within the large feasible domain obtained earlier, the objective function is examined using the simple exhaustive search and curve fitting techniques. Automation of the optimization procedure is achieved using univariate search and Golden-section scheme. The optimal drawing conditions, defined by draw speed and draw temperature, and optimal furnace dimension are obtained for given constraints. The observations during intermediate evaluations are also discussed in terms of the physical characteristics of the process.

Acknowledgements

The authors acknowledge the financial support provided by the National Science Foundation, under Grant DMI-96-33194, and the computing resources provided by the National Computational Science Alliance (NCSA). The partial support by the Center for Computational Design (CCD) at Rutgers University is also acknowledged. The discussions with Prof. C.E. Polymeropoulos are gratefully acknowledged.

References

[1] T. Li (Ed.), Optical Fiber Communications, Vol. 1: Fiber Fabrication, Academic Press, Orlando, FL, 1985.
[2] U.C. Paek, Free drawing and polymer coating of silica glass optical fibers, ASME J. Heat Transfer 121 (1999) 774–788.
[3] Y. Jaluria, Heat and mass transfer in the thermal processing of advanced materials, Heat Transfer 1998, Proc. 11th IHTC, Taylor & Francis, Philadelphia, PA, 1 (1998) 189–211.
[4] M. Nicolardot, G. Orcel, Numerical simulation of optical fiber preform neck-down for draw process optimization, International Wire & Cable Symposium Proceedings (1999) 369–376.
[5] X. Cheng, Y. Jaluria, Feasible domain of high speed optical fiber drawing, ASME J. Heat Transfer 126 (2004) 852–857.
[6] C.A. Mirho, Computer-assisted control of an optical fiber draw tower, MS thesis, Rutgers University, New Brunswick, NJ, 1990.
[7] W.K.S. Chiu, Y. Jaluria, N.G. Glumac, Control of thin film growth in chemical vapor deposition manufacturing systems, ASME J. Mfg. Sci. Eng. 124 (2002) 715–724.
[8] E.M. Dianov, V.V. Kashin, S.M. Perminov, V.N. Perminova, S. Ya Runanov, S.M. Sysoev, The effects of different conditions on the drawing of fibers from preforms, Glass Tech. 29 (1988) 258–262.
[9] V.N. Vasilijev, G.N. Dulnev, V.D. Naumchic, The flow of highly viscous liquid with a free surface, Glass Tech. 30 (1989) 83–90.
[10] Z. Wei, K.-M. Lee, S.W. Tchikanda, Z. Zhou, S.-P. Hong, Free surface flow in high speed fiber drawing with large-diameter preforms, ASME J. Heat Transfer 126 (2004) 713–722.
[11] Z.H. Xiao, Flow, heat transfer, and free-surface shape during the optical fiber drawing process, PhD thesis, Rensselaer Polytechnic Institute, Troy, New York, 1997.
[12] S.H.-K. Lee, Y. Jaluria, Geometry and temperature variations on the radiative transport during optical

fiber drawing, J. Mater. Process. Mfg. Sci. 3 (1995) 317–331.
[13] S. Roy Choudhury, Y. Jaluria, Practical aspects in the drawing of an optical fiber, J. Mater. Res. 13 (1998) 483–493.
[14] Z. Yin, Y. Jaluria, Thermal transport and flow in high-speed optical fiber drawing, ASME J. Heat Transfer 120 (1998) 916–930.
[15] S.H.-K. Lee, Y. Jaluria, Simulation of the transport processes in the neck-down region of a furnace drawn optical fiber, Int. J. Heat Mass Transfer 40 (1997) 843–856.
[16] R. Sayles, B. Caswell, A finite element analysis of the upper jet region of a fiber drawing flow field, Int. J. Heat Mass Transfer 27 (1984) 57–67.
[17] M.R. Myers, A model for unsteady analysis of preform drawing, AIChE J. 35 (1989) 592–602.
[18] Z. Yin, Y. Jaluria, Zonal method to model radiative transport in an optical fiber drawing furnace, ASME J. Heat Transfer 119 (1997) 597–603.
[19] S. Roy Choudhury, Y. Jaluria, Thermal transport due to material and gas flow in a furnace for drawing an optical fiber, J. Mater. Res. 13 (1998) 494–503.
[20] H. Hanafusa, Y. Hibino, F. Yamamoto, Formation mechanism of drawing-induced E'centers in silica optical fibers, J. Appl. Phys. 58 (1985) 1356–1361.
[21] S. Roy Choudhury, Y. Jaluria, S.H.-K. Lee, Generation of neck-down profile for furnace drawing of optical fiber, Numer. Heat Transfer 35 (1999) 1–24.
[22] Z. Yin, Y. Jaluria, Neckdown and thermally induced defects in high speed optical fiber drawing, ASME J. Heat Transfer 122 (2000) 351–362.
[23] Y. Jaluria, K.E. Torrance, Computational Heat Transfer, second ed., Taylor & Francis Pub. Co., New York, 2003.
[24] Y. Jaluria, Thermal processing of materials: From basic research to engineering, ASME J. Heat Transfer 125 (2003) 957–979.
[25] Y. Jaluria, Fluid flow phenomena in materials processing—The 2000 freeman scholar lecture, ASME J. Fluids Eng. 123 (2001) 173–210.
[26] S. Sakaguchi, Drawing of high-strength long-length optical fibers for submarine cables, IEEE J. Lightwave Technol. LT-2 (1984) 808–815.
[27] Y. Jaluria, Design and Optimization of Thermal Systems, McGraw-Hill, New York, 1998.
[28] G.N. Vanderplaats, Numerical Optimization Techniques for Engineering Design with Applications, McGraw-Hill, 1984.
[29] W.F. Stoecker, Design of Thermal Systems, third ed., McGraw-Hill, 1989.
[30] J.S. Arora, Introduction to Optimum Design, McGraw-Hill, New York, 1989.
[31] X. Cheng, Y. Jaluria, Effect of draw furnace geometry on high-speed optical fiber manufacturing, Numer. heat Transfer 41 (2002) 757–781.